

THE 492 GHz ATMOSPHERIC OPACITY AT THE GEOGRAPHIC SOUTH POLE

RICHARD A. CHAMBERLIN¹

Department of Astronomy, Boston University, 725 Commonwealth Avenue, Boston, MA 02215

AND

ADAIR P. LANE AND ANTONY A. STARK

Harvard-Smithsonian Center for Astrophysics, 60 Garden Street, MS-78, Cambridge, MA 02138

Received 1996 May 16; accepted 1996 August 20

ABSTRACT

We present narrow-bandwidth submillimeter-wave sky opacity measurements made from the South Pole between 1995 February 9 and November 17, a period that includes an entire Austral winter. These measurements were made with the Antarctic Submillimeter Telescope and Remote Observatory (AST/RO) using a heterodyne receiver tuned to a band that includes the 492 GHz fine-structure line of neutral atomic carbon. The zenith optical depth was below 0.72 half the time during the Austral winter and spring, and it reached values as low as 0.34 on day 232. The stability was also remarkably good: the opacity remained below 1.0 for weeks at a time. The South Pole is therefore an excellent site for submillimeter astronomy throughout the Austral winter and spring. The functional relationship between 492 GHz opacity and measured precipitable water vapor shows that a significant fraction of the opacity is caused by atmospheric constituents other than water vapor, indicating the need for accurate, site-dependent atmospheric modeling when opacity measurements at lower frequencies are extrapolated into the submillimeter.

Subject headings: atmospheric effects — Earth — methods: observational —
radio continuum: general — site testing

1. INTRODUCTION

Submillimeter astronomy can only be done from high, dry sites where the water vapor content of Earth's atmosphere is low. The US Amundsen-Scott South Pole Station is located at 2835 m altitude on the Antarctic Plateau, and it is among the coldest and driest places on Earth. The low water vapor content of the South Pole sky, as determined from several decades of routine weather measurements, is thought to make the South Pole an outstanding site for infrared, millimeter, and submillimeter astronomy. A long history of water vapor column measurements and sky brightness measurements at various wavelengths support this expectation (Smythe & Jackson 1977; Dragovan et al. 1990; Chamberlin & Bally 1994, 1995; Chamberlin 1995).

In this paper, we present submillimeter-wave opacity data obtained in 1995 that show the excellent quality of the South Pole as an astronomical site. We compare measured opacities with total water vapor column measured by other means, to show that not all of the observed opacity is caused by water vapor. In conclusion, we discuss the implications of the South Pole data for submillimeter-wave site testing at other locations.

2. OBSERVATIONAL METHOD

Narrow-bandwidth submillimeter-wave opacity measurements were made from the South Pole with the newly installed Antarctic Submillimeter Telescope and Remote Observatory (AST/RO) (Stark et al. 1994; Lane & Stark 1995; Stark et al. 1996). A double-sideband, quasi-optical SIS receiver (Engargiola, Zmuidzinas, & Lo 1994) was used, with an intermediate frequency (IF) of 1.5 GHz and an IF

bandwidth of ~ 700 MHz. The gains in the two sidebands are essentially equal. The receiver was tuned in such a way that one of the sidebands was centered on 492.16 GHz—the rest frequency of the $^3P_1 \rightarrow ^3P_0$ fine-structure transition of neutral atomic carbon—because this work was carried out in conjunction with Galactic survey observations of this line. From 1995 February 9 (day 40) through May 17 (day 137), the receiver was tuned in such a way that the carbon line was in the upper sideband; it was subsequently retuned to place the line in the lower sideband, in order to reduce the total system noise by placing the image sideband at a frequency at which the sky is more transparent.

The data presented here cover the period from 1995 February 9 (day 40) to November 17 (day 321). This period includes the 6 month long South Pole night, days 81–267. Opacity was measured using a “skydip” technique: the antenna temperature difference between the sky and a calibrated cold load was measured sequentially at 14 elevation angles corresponding to air masses from 1.2 to 3.8, with an interval of 0.2 air mass ($= 1 \sin^{-1}$ [elevation]). Normally, one or more skydips were performed each day regardless of prevailing weather conditions, except when the surface wind speed exceeded $\sim 10 \text{ m s}^{-1}$, which was 5% of the time. On a few days, measurements were not possible for logistical and maintenance reasons. During the observing season, over 1100 individual skydips were obtained, usually in groups of three, and each skydip took about 5 minutes to complete.

To obtain an opacity value from each skydip, the set of measured antenna temperatures, $T_{\text{sky}}(A)$, was fitted to a single-slab model of the atmosphere (cf. Ulich & Haas 1976):

$$T_{\text{sky}}(A) = C - B \exp(-\tau_0 A), \quad (1)$$

$$C \equiv \eta_l J(v, T_{\text{atm}}) + (1 - \eta_l) J(v, T_{\text{str}}), \quad (2)$$

¹ Current address: California Institute of Technology, Submillimeter Observatory, 111 Nowelo Street, Hilo, HI 96720.

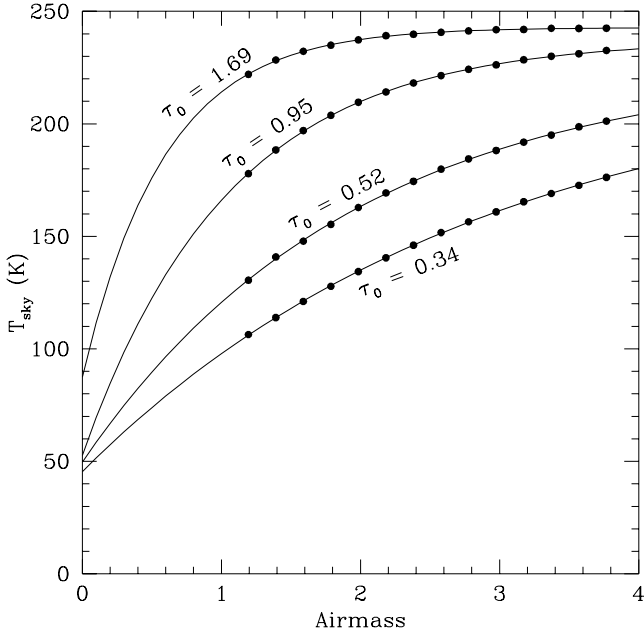


FIG. 1.—Four skydip observations in different opacity conditions. Lines are fits of eq. (1) to the data.

$$B \equiv \eta_l [J(\nu, T_{\text{atm}}) - J(\nu, T_{\text{bg}})], \quad (3)$$

$$J(\nu, T) \equiv \frac{h\nu/k}{\exp(h\nu/kT) - 1}, \quad (4)$$

where A is the air mass, $J(\nu, T)$ is the effective radiation temperature of a blackbody source at temperature T observed at frequency ν , T_{atm} is the mean atmospheric temperature, T_{sbr} is the apparent brightness temperature of the spillover and radiation losses, $T_{\text{bg}} = 2.7$ K is the background temperature of space, η_l is the telescope efficiency, and τ_0 is the zenith atmospheric opacity. We have assumed that any elevation angle dependencies of T_{sbr} and η_l may be ignored, and that the two sidebands may be combined. Each skydip was fitted to equation (1) by χ^2 minimization, leaving τ_0 , B , and C as free parameters. For these data, no a priori knowledge of τ_0 , B , or C was required because τ_0 was in an intermediate regime ($0.2 < \tau_0 < 2$), where equation (1)

is significantly nonlinear for $1 < A < 4$; the χ^2 minimization routine therefore had no difficulty finding stable and unique fits for τ_0 , B , and C . The minimum χ^2 values obtained were often near 11—the value expected from the number of degrees of freedom in the fit and the errors in the T_{sky} measurements ($\sigma \simeq 0.2$ K)—showing that the data are consistent with our model and, in particular, that T_{sbr} and η_l do not vary significantly with elevation angle. At other times, the minimum χ^2 value was large because the sky brightness deviated from a single-slab atmospheric model, e.g., in cloudy weather. The C and B values found in the fits, $C \sim 230$ K and $B \sim 175$ K, were consistent with our independent knowledge of C and B based on observations of the Moon, which indicated that $\eta_l \geq 0.75$, and calculations of T_{atm} from balloon-borne radiosonde data, which indicated that $220 \leq T_{\text{atm}} \leq 244$ K.

Four fits, under different opacity conditions, are shown in Figure 1. The noise in the T_{sky} measurements is less than the size of the dots. Note that the deviations of the data from the model fits (*solid lines*) are small. At large values of the air mass A , T_{sky} approaches the value C , which is approximately T_{atm} . The extrapolation of the model to $A = 0$ yields $T_{\text{sky}} = C - B$, which is $(1 - \eta_l)T_{\text{sbr}} \approx 0.25T_{\text{ambient}}$.

3. RESULTS AND DISCUSSION

Figure 2 shows zenith opacity determined from skydip measurements as a function of day number in 1995. The line connects values determined from over 1100 skydips. The opacity applicable to observations of the 492 GHz carbon line is somewhat overestimated prior to day 137, when the local oscillator (LO) was set to place the line in the upper sideband rather than the lower (see below).

Figure 3 shows a cumulative distribution function for τ_0 during the winter/spring period, days 100–321. Opacities were measured for a total of 171 days out of a possible 222 days during this period, which was the driest period during the year. The 492 GHz opacity “quartiles” from the data in Figure 3 are presented in Table 1, with separate columns for the winter/spring and summer periods.

The effects of possible bias in our results due to incomplete sampling can be estimated using concurrent water vapor data obtained by the South Pole meteorology office. Figure 4 shows a plot of the 492 GHz opacity versus the

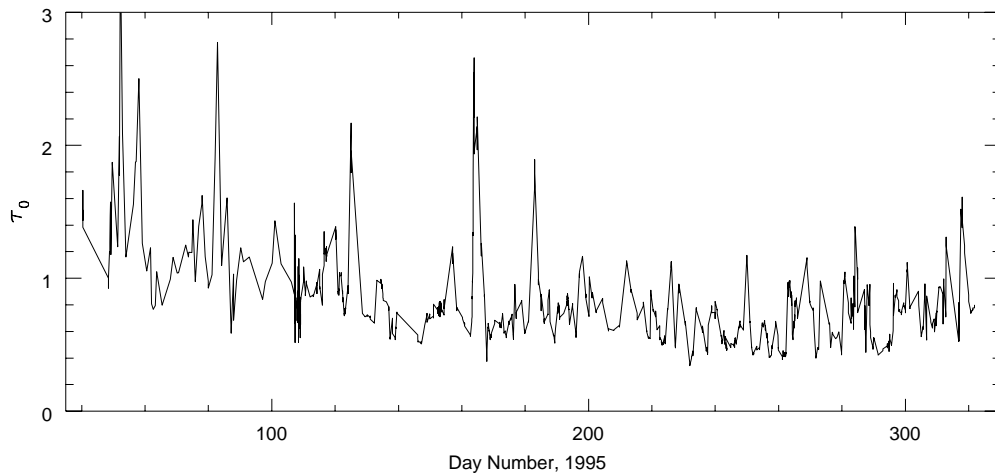


FIG. 2.—South Pole zenith opacity at 492 GHz as a function of day number in 1995. Solid line connects values measured from 1158 individual skydip observations. Prior to day 137, the LO center frequency was 490.66 GHz; after day 137, the center frequency was 493.66 GHz.

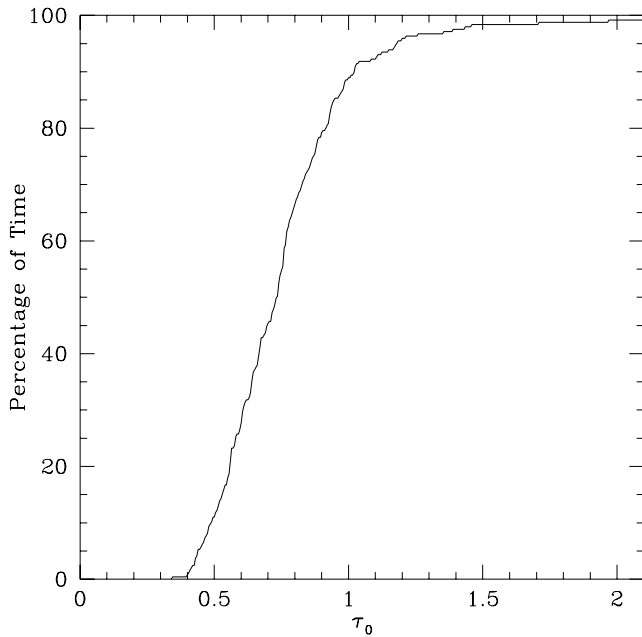


FIG. 3.—Cumulative distribution function of observed 492 GHz opacities during the winter/spring period (day 100 to day 321). The percentage of time the opacity was less than a given value is plotted versus the value of τ_0 .

column of precipitable water vapor (PWV) determined by radiosonde. Each point represents a single skydip measurement correlated with a balloon sounding made within ± 6 hr of the skydip observation. Our method of deriving PWV from radiosonde measurements, as well as a discussion of possible errors in this determination, was described previously by Chamberlin & Bally (1995). The data in Figure 4 were fitted by a least-squares method to

$$\tau_0 = a + b\text{PWV}, \quad (5)$$

where a is the dry air opacity and b is the dependence of the zenith opacity on water vapor abundance. As shown in Figure 4, the dry air opacity a differs for the two placements of the image sideband, being higher for the lower frequency tuning, which is closer to a major O_2 emission-line core centered on 487.25 GHz. Opacity values derived from the earlier, lower frequency tuning (day 40 to day 137) are represented as crosses, and the broken line is a least-squares fit of equation (5) to these data. From the fit, $a = 0.57$ per air mass, and $b = 1.44$ per air mass per $\text{mm}_{(\text{H}_2\text{O})}$. Opacity values derived from the later, higher frequency tuning (day

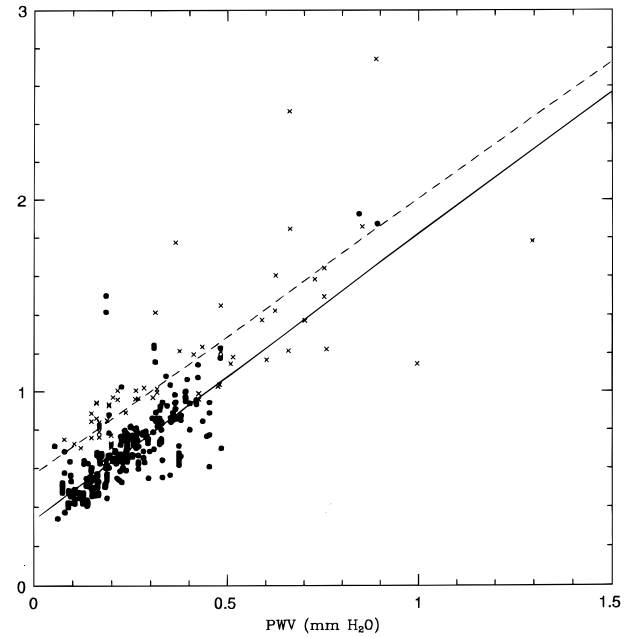


FIG. 4.—492 GHz zenith opacity, obtained from AST/RO skydip measurements, plotted as a function of precipitable water vapor, as determined by balloon radiosonde. Crosses: 490.66 GHz opacity; dashed line is the best fit of eq. (5), with $a = 0.57$, $b = 1.44$. Solid circles: 493.66 GHz opacity; solid line is the best fit of eq. (5), with $a = 0.33$, $b = 1.49$.

137 to day 321) are represented as solid circles, and the solid line is a least-squares fit to these data: from the fit, $a = 0.33$ per air mass; $b = 1.49$ per air mass per $\text{mm}_{(\text{H}_2\text{O})}$.

Table 2 shows a comparison of our measured values for a and b with the predictions obtained from the Grossman atmospheric transparency model (Grossman 1989). For both receiver tunings, the model significantly underpredicts a . The model's agreement with the empirically determined b is better. The discrepancy between the model and the experimental value for a is much larger for the 493.66 GHz LO tuning, which is more distant from the 487.25 GHz O_2 line core.

Since daily radiosonde measurements were made, and since we have shown (see Fig. 4) that the 492 GHz opacity is correlated with the radiosonde-derived PWV values, it is possible to use the radiosonde measurements made on days the telescope did not perform skydips to estimate how our statistics may be affected by incomplete sampling. We used the τ_0 -PWV relation obtained from the higher frequency tuning ($a = 0.33$, $b = 1.49$) to estimate the opacity for 51

TABLE 1
SUBMILLIMETER OPACITY AND PWV QUANTILES FOR SOUTH POLE STATION

QUANTILE (%)	SUMMER ^a			WINTER/SPRING ^b		
	PWV ^c	$\tau_0(225 \text{ GHz})^d$	$\tau_0(492 \text{ GHz})^e$	PWV ^c	$\tau_0(225 \text{ GHz})^d$	$\tau_0(492 \text{ GHz})^f$
25	0.43	0.056	0.96	0.19	0.040	0.60
50	0.54	0.068	1.14	0.25	0.048	0.72
75	0.72	0.080	1.40	0.32	0.057	0.86
99	1.50	0.153	2.57	0.89	0.099	2.07

^a Days 1–99 and days 322–365.

^b Days 100–321.

^c Precipitable water vapor in millimeters, calculated from radiosonde.

^d Data from Chamberlin & Bally 1994, 1995.

^e This paper. Missing data estimated using $\tau_0(492 \text{ GHz})$ —PWV relation in Fig. 4.

^f This paper. From skydip observations on 171 out of 222 days.

TABLE 2
MODEL AND EXPERIMENTAL COEFFICIENTS a AND b

LO TUNING (GHz)	GROSSMAN AT MODEL		EXPERIMENTAL	
	a	b	a	b
490.66	0.38	$1.37 < b < 1.59$	0.57 ± 0.06	1.44 ± 0.12
493.66	0.086	$1.22 < b < 1.50$	0.33 ± 0.02	1.49 ± 0.07
225 ^a	$0.003 < a < 0.007$	$0.032 < b < 0.12$	0.030 ± 0.001	0.069 ± 0.002

^a Data from Chamberlin & Bally 1995.

missing days during the winter/spring period. Recomputing the opacity cumulative distribution function, with the inclusion of the estimated opacities for the missing days, gives quartile values of 0.60, 0.73, 0.84, and 2.07, negligibly different from the observed values listed in the last column of Table 1. Thus, we are confident that our statistics were not significantly biased by the incomplete sampling.

Figure 5 shows the estimated opacity for every day of the year using the τ_0 -PWV relation from the 493.66 GHz tuning. The averaged daily opacities actually measured with this tuning are shown as solid circles in the figure. We used these daily estimates of the opacity to predict the cumulative distribution function we would have measured if the receiver was operational with this tuning during the whole "summer" period, which is a period of relatively high water vapor. The quartile data derived from this cumulative distribution function are listed in the fourth column of Table 1.

The stability of the South Pole atmosphere during low-opacity periods is remarkable. In Figure 6, we present a time series of opacity measurements taken over a 1.3 day period. Each point represents the opacity derived from an individual skydip measurement. The peak scatter of these opacity values during this period was less than $\pm 10\%$. The

initial 0.4 days of the measured period shows a peak scatter of less than $\pm 4\%$. Such atmospheric stability is important for the detection of faint spectral lines, low-level continuum sources, and cosmic microwave background anisotropy. In addition, this excellent temporal stability in τ_0 implies that detection over exceptionally large coherence areas may be practical with submillimeter interferometric instruments.

The periods of lowest water vapor also tend to have low wind speeds. Wind velocity and precipitable water vapor at the South Pole exhibit correlated behavior (Schwerdtfeger 1984) with two distinct patterns. The usual weather pattern consists of dry, inversion-driven winds of about 5.5 m s^{-1} from the interior of the Antarctic plateau. This is punctuated by periods of horizontal advection of warm, relatively moist maritime air manifested in a westerly shift in wind direction and an increase in wind speed of $\sim 3 \text{ m s}^{-1}$. The highest wind speed at the South Pole between 1957 and 1983 was 24 m s^{-1} , and there are many months during which the wind speed does not exceed 12 m s^{-1} (Schwerdtfeger 1984). Our experience was that essentially all the acceptable submillimeter-wave observing weather occurs when wind speeds are under 10 m s^{-1} . This regime of wind speeds less than 10 m s^{-1} prevailed 95% of the time in

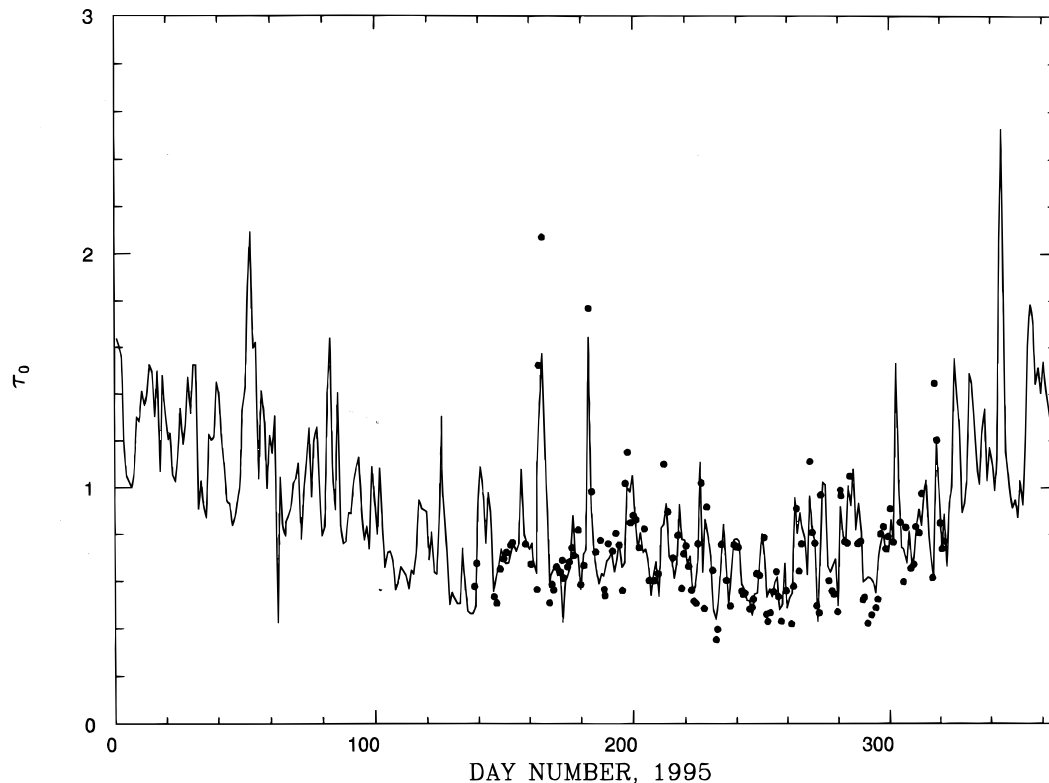


FIG. 5.—Solid line shows the time series for the whole year of 492 GHz opacities estimated from daily radiosonde data and the τ_0 -PWV relation shown in Fig. 4 (493 GHz tuning). Averaged daily opacities measured using skydips with this tuning are shown as solid circles.

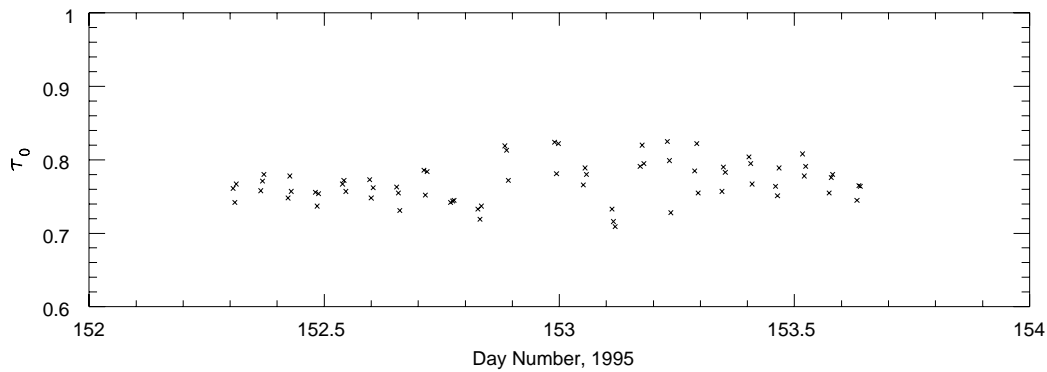


FIG. 6.—Detailed time series of opacities derived from individual skydips, showing great stability

1995. Low wind conditions are unusually favorable for the construction of large telescopes, where maximum wind speed determines the survival strength of the structure, and maximum wind speed during observations determines the required stiffness.

4. CONCLUSION

The results presented here constitute the first systematic, long-term measurements of submillimeter-wave atmospheric opacity at an astronomical site. These measurements have been made in conjunction with balloon-borne PWV measurements, which have allowed us to determine the relative contributions to the opacity from dry air and from water vapor. We have shown that (1) the South Pole is an excellent submillimeter site even at a frequency of 492 GHz, which is on the wing of a strong atmospheric O_2 line, and (2) that a significant fraction of the opacity at this frequency is the result of dry air.

Our results have implications for the testing of other sites. In the absence of direct measurements of submillimeter-wave opacity, the opacity at lower frequencies (millimeter wavelengths) has often been used to try to predict the submillimeter-wave opacity (e.g., Stevens & Robson 1994; Masson 1994). On Mauna Kea, for example, the relation $\tau_{492 \text{ GHz}} \approx 20(\tau_{225 \text{ GHz}} - 0.01)$ is often used: $\tau_{225 \text{ GHz}}$ is used as a measure of PWV, which is then assumed to be the dominant source of opacity at 492 GHz. For the South Pole, a site with extremely low water vapor, we find that the effect of dry air opacity must be taken into account. Further, we note that the dry air opacity can depend strongly on the elevation of the site and is not well predicted by existing atmospheric models (Chamberlin & Bally 1995). If we compare the values of b , relating opacity to PWV in equation (5), for the 492 GHz data from the present work and the 225 GHz data from Chamberlin & Bally (1995), we find $b_{492 \text{ GHz}}/b_{225 \text{ GHz}} = 21$ —comparable with the value of

20 seen on Mauna Kea. Since the effect of dry air opacity cannot be calculated with accuracy, there is no reliable substitute for actual submillimeter-wave measurements when testing site quality.

To date, the three best sites where 225 GHz opacity measurements have been made are South Pole, Mauna Kea, and the proposed Millimeter Array site in the Atacama desert in Chile; the data obtained at each site using similar National Radio Astronomy Observatory tipping radiometers are summarized in Table 3. The data have been divided into the best 6 month period and the remainder of the year. All three sites exhibit superb millimeter-wave opacity. The extrapolation of the 225 GHz opacity into the submillimeter is problematic, since the relative contribution of water vapor and of other atmospheric constituents is site-dependent and varies with wavelength. On Mauna Kea and Atacama, the water vapor content of the atmosphere is usually several times that of the South Pole, but the dry air opacity contribution is smaller because the altitude is significantly higher. Since 492 GHz measurements have been compared with 225 GHz measurements at Mauna Kea, the 225 GHz site testing can be quantitatively extrapolated to 492 GHz (Masson 1994), and it is compared to our 492 GHz measurements in Table 4. Submillimeter sky opacity and noise depends on atmospheric pressure, temperature, and PWV. Of the three sites, South Pole consistently has the lowest PWV and temperature but the highest pressure. This mixture makes the South Pole comparatively better at some wavelengths than at others; in particular, the transparency at wavelengths near 350 and 450 μm is sensitive to PWV, favoring the Pole.

We have shown that the submillimeter-wave sky conditions at the South Pole during the Austral winter are extremely favorable compared to any other site where measurements have been made. Even at the problematic frequency of 492 GHz, which shows significant opacity from

TABLE 3
225 GHz ZENITH OPACITY (NRAO TIPPER DATA)

QUARTILE (%)	SOUTH POLE ^a		MAUNA KEA ^b		ATACAMA ^c	
	92 Apr-Sep	Other, 1992	Jan-Jun	Jul-Dec	95 Apr-Sep	95 Oct-96 Mar
25	0.040	0.052	0.052	0.079	0.032	0.046
50	0.046	0.062	0.076	0.129	0.044	0.077
75	0.055	0.076	0.136	0.245	0.066	0.138

^a Data from Chamberlin & Bally 1994, 1995.

^b Data from Hogg 1992, averaged over the period from 1989 October 1 to 1991 August 31.

^c Data from Scott Foster (1996, private communication).

TABLE 4
492 GHz ZENITH OPACITY

QUARTILE (%)	SOUTH POLE ^a		MAUNA KEA ^b	
	Apr-Sep	Oct-Mar	Jan-Jun	Jul-Dec
25	0.55	0.84	0.84	1.38
50	0.70	1.03	1.32	2.38
75	0.81	1.33	2.52	4.70

^a This paper, with quartiles computed equinox to equinox.

^b Extrapolated from the 225 GHz data in Table 3 using the relation: $\tau_{492 \text{ GHz}} \approx 20(\tau_{225 \text{ GHz}} - 0.01)$ (Masson 1994).

the dry-air continuum and the oxygen line at 487 GHz, the low water vapor column above South Pole allows submillimeter-wave observations continuously throughout most of the year. During the best observing period, Austral winter and spring, the zenith opacity at 492 GHz was below

1.0 over 85% of the time. Such observing conditions are unprecedented.

We thank the South Pole meteorology office. We thank our collaborators at Bell Laboratories, Boston University, California Institute of Technology, University of Cologne, University of Colorado, and University of Illinois, who have contributed to the success of AST/RO. We thank Tom Phillips and Colin Masson for helpful discussions. We are grateful for the support of the 1995 South Pole winter-over crew, Antarctic Support Associates, and the National Science Foundation. This research was supported in part by the National Science Foundation (NSF) under grant OPP 88-18384, and under a cooperative agreement with the Center for Astrophysical Research in Antarctica (CARA), grant NSF OPP 89-20223. CARA is an NSF Science and Technology Center.

REFERENCES

- Chamberlin, R. A. 1996, *Antarctic J. US*, 30(5), 342
 Chamberlin, R. A., & Bally, J. 1994, *Appl. Opt.*, 33(6), 1095
 ———. 1995, *Int. J. Infrared Millimeter Waves*, 16(5), 907
 Dragovan, M., Stark, A. A., Pernic, R., & Pomerantz, M. A. 1990, *Appl. Opt.*, 29(4), 463
 Engargolia, G., Zmuidzinas, J., Lo, K.-Y. 1994, *Rev. Sci. Instrum.*, 65, 1833
 Grossman, E. 1989, A T program, Ver. 1.5, Air Head Software, 2069 Bluff St., Boulder, CO 80302, unpublished
 Hogg, D. E. 1992, Millimeter Array Memo No. 79
 Lane, A. P., & Stark, A. A. 1996, *Antarctic J. US*, 30(5), 377
 Masson, C. R. 1994, in *ASP Conf. Ser. 59, Astronomy with Millimeter and Submillimeter Wave Interferometry*, ed. M. Ishiguro & W. J. Welch (San Francisco: ASP), 87
 Schwerdtfeger, W. 1984, *Weather and Climate of the Antarctic* (Amsterdam: Elsevier), 182
 Smythe, W. D., & Jackson, B. V. 1977, *Appl. Opt.*, 16(8), 2041
 Stark, A. A., Chamberlin, R. A., Cheng, J., Ingalls, J., & Wright, G. 1996, *Rev. Sci. Instrum.*, in press
 Stark, A. A., et al. 1994, *Antarctic J. US*, XXIX(5), 344
 Stevens, J. A., & Robson, E. I. 1994, *MNRAS*, 270, L75
 Ulich, B. L., & Haas, R. W. 1976, *ApJS*, 30, 247